Asok Ray
Fellow ASME

Min-Kuang Wu

Marc Carpino

Department of Mechanical Engineering,
The Pennsylvania State University,
University Park, PA 16802

Carl F. Lorenzo
NASA Lewis Research Center,
Cleveland, OH 44135

Damage-Mitigating Control of Mechanical Systems: Part II—Formulation of an Optimal Policy and Simulation[1]

The objective of damage-mitigating control introduced in the first part of this two-part paper is to achieve high performance without overstraining the mechanical structures. The major benefit is an increase in the functional life of critical plant components along with enhanced safety, operational reliability, and availability. Specifically, a methodology for modeling fatigue damage has been developed as an augmentation to control and diagnostics of complex dynamic processes such as advanced aircraft, spacecraft, and power plants. In this paper which is the second part, an optimal control policy is formulated via nonlinear programming under specified constraints of the damage rate and accumulated damage. The results of simulation experiments for upthrust transient operations of a reusable rocket engine are presented to demonstrate efficacy of the damage-mitigating control concept.

1 Introduction

The motivation and concept of damage-mitigating control (*DMC*) have been introduced in the first part (Ray et al., 1993) of this two-part paper. The objective of *DMC* is to achieve high performance without overstraining the mechanical structures in complex dynamic systems such as advanced aircraft, spacecraft, and power plants; and the major benefit is an increase in the functional life of critical plant components along with enhanced safety, operational reliability, and availability. In the first part, a structure for the damage-mitigating control system is proposed, and a methodology is formulated to model fatigue damage in the continuous-time setting instead of the standard practice of cycle-based damage representation. This damage model can be conveniently concatenated with the plant dynamic model, and is specifically suited to synthesis of a control policy where the damage rate and accumulated damage are constrained or embedded within the cost functional.

In many applications such as start-up of the space shuttle main engine (Sutton, 1992), take-off and landing of aircraft, and start-up and scheduled shutdown of power plants, the control system may consist of an open-loop (feedforward) policy to steer the plant along a nominal trajectory and a closed loop (feedback) policy to compensate for deviations from the normal trajectory. In that case, the active controller, as proposed in Fig. 1 of the first part, is to be synthesized using the principles of mathematical programming, optimal state estimation and state feedback. At the same time, the control system must satisfy the inequality constraints imposed by the continuous-time damage model such that the prescribed limits of damage rate and accumulated damage are not exceeded. This paper, which is the second part, presents the synthesis of an optimal policy for open-loop control based on the nominal plant model and damage constraints. Synthesis of a closed-loop control policy for robust compensation of modeling uncertainties and disturbances is a subject of current research, and the basic concept is outlined in Appendix A. The benefits of damage mitigation and efficacy of the proposed damage-mitigating control are demonstrated via simulation of a reusable rocket engine. The results of simulation experiments reveal that, during upthrust transients, a substantial gain in the service life of the turbopump can be achieved without any appreciable loss of engine dynamic performance.

[1]The research work reported in this paper is supported in part by: NASA Lewis Research Center under Grant No. NAG 3-1240; National Science Foundation under Research Grant No. ECS-9216386; Electric Power Research Institute under Contract EPRI RP8030-5; Office of Naval Research under Grant No. N00014-90-J-1513; National Science Foundation under Equipment Grant No. MSS-9112609.

Contributed by the Dynamic Systems and Control Division for publication in the JOURNAL OF DYNAMIC SYSTEMS, MEASUREMENT, AND CONTROL. Manuscript received by the DSCD September 16, 1992; revised manuscript received April 20, 1993. Associate Technical Editor: J. Stein.

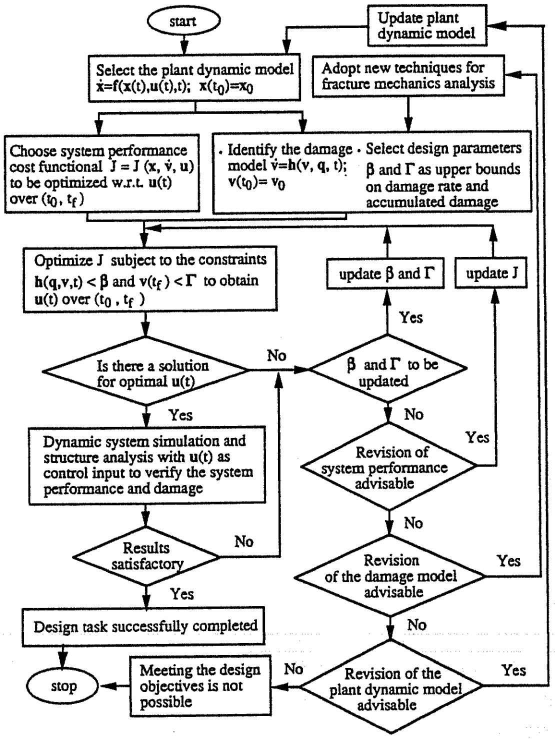

Fig. 1 Nonlinear programming procedure for generating the open-loop control policy

In addition to the improvement in service life, on-line damage prediction could be utilized for prognosis of impending failures of critical plant components to enhance plant and personnel safety, improve availability and operability, and reduce operational cost. Therefore, the damage-mitigating control and failure prognosis system can be made to be an integral part of the (hierarchically structured) intelligent decision and control system (Shoureshi and Wormley, 1990; Lorenzo and Merrill, 1991) that must be tolerant of the following:

- A variety of errors resulting from parametric and nonparametric uncertainties in plant modeling, and continuously varying or discrete-event disturbances;
- The accumulated damage over the period between consecutive maintenance actions.

Failure prognosis and risk assessment based on on-line damage prediction requires stochastic modeling of the damage dynamics, which is an extension of the work reported in the first part. This is also a subject of current research, and the basic issues in failure prognosis and probabilistic risk assessment are outlined in Appendix B.

This second part is organized in four sections including the Introduction and two Appendices. Section 2 is devoted to the development of an optimal policy for open-loop control of the plant under specified constraints of damage rate and accumulated damage. Appendix A outlines a policy for closed loop control to steer the plant along the nominal trajectory of open-loop control. Appendix B discusses how the predicted damage can be used for failure prognosis and condition-based risk analysis. Section 3 presents the results of simulation experiments for transient operations of a reusable rocket engine under open-loop control. This two-part paper is concluded in Section 4.

2 Open-Loop Control Policy Via Nonlinear Programming

The dynamics of the plant under control and the fatigue damage of the structural components are modeled, within the domain of the plant operating range, by the nonlinear (and possibly time-varying) differential equations as depicted in the first part. For ease of reference, the structures of these models are presented below:

Task period: Starting time t_0 to final time t_f

Plant dynamics:
$$\frac{dx}{dt} = f(x(t),u(t),t);\ x(t_0) = x_0 \tag{1}$$

Damage dynamics:
$$\frac{dv}{dt} = h(v(t),q(x,t),t);\ v(t_0) = v_0;\ h \geq 0\ \ \forall t \tag{2}$$

where $x \in \mathbf{R}^n$ is the plant state vector; $u \in \mathbf{R}^m$ is the control input vector; $v \in \mathbf{R}^r$ is the damage state vector; $q \in \mathbf{R}^p$ is the load vector as explained in the first part; and Eqs. (1) and (2) must satisfy the local Lipschitz condition (Vidyasagar, 1992).

Given an initial condition, the open-loop control policy is obtained via nonlinear programming (Luenburger, 1984) by minimizing a specified cost functional under the prescribed constraints of damage rate and accumulated damage as discussed in the first part. The objective is to minimize the cost functional J (which includes plant state, damage rate, and control input vectors) without violating the upper bounds of damage rate and accumulated damage. The cost functional J is to be chosen in an appropriate form.

$$\text{Minimize: } J = \sum_{k=0}^{N-1} J_k(\tilde{x}_k, \dot{v}_k, \tilde{u}_k) \tag{3}$$

$$\text{Subject to: } (v_N - v_0) < \Gamma \text{ and } 0 \leq h(v_k, q(x_k), k) < \beta(k)$$
$$\text{for } k = 1,2,3,\cdots,N \tag{4}$$

where $\tilde{x}_k = x_k - x_{ss}$ and $\tilde{u}_k = u_k - u_{ss}$ are deviations of the plant state vector and the control input vector from the respective final steady state values of x_{ss} and u_{ss}; and $\beta(t) \in \mathbf{R}^r$ and $\Gamma \in \mathbf{R}^r$ are specified tolerances for the damage rate and accumulated damage, respectively.

The open-loop control law was synthesized by minimizing the cost functional in Eq. (3) under: (i) the above inequality constraints in Eq. (4); and (ii) the condition that, starting from the initial conditions $x(t_0)$ and $v(t_0)$, the state trajectory must satisfy the plant dynamic model in Eq. (1). The design variables to be identified are the control inputs u_k, $k = 0,1,2,\cdots, N-1$ and the goal is to search for an optimal control sequence $\{u_k\}$. The flow chart shown in Fig. 1 depicts the procedure for open-loop control synthesis via nonlinear programming. The basic features of this optimization procedure are described in the following.

A mathematical model of the plant dynamics is formulated in the state space form of Eq. (1) with proper initial conditions. Based on the responses of the plant at the normal operating condition, the critical component(s) in which damage is most likely to occur is (are) identified either by stress analysis or from the history of plant operations. Upon identification of the critical points for damage prediction, the structural dynamic modeling and the continuous-time damage modeling, as described in the first part, are used to formulate the damage dynamics in Eq. (2). The resulting damage rate and accumulated damage are to be constrained in the optimization procedure. The upper bounds of the constraints on damage rate and accumulated damage need to be appropriately chosen by taking the mission objectives, the time interval between maintenance actions, service life and allowable risk into consideration. The initial damage is important due to its significant effects on the dynamics of damage accumulation. The cost functional in Eq. (3) is a function of the plant state and damage rate vector, representing a trade-off between system performance and damage. The weights are to be assigned to the plant states or selected output variables reflecting their relative impact on the system performance. If the damage constraints are appropriately chosen, it may not be necessary to include the damage rate in the cost functional.

The task is now to formulate an optimal control sequence $\{u_k\}$ from time t_0 to t_f based on the cost functional, the models of plant and damage dynamics, and the damage constraints. This optimal control sequence is then tested via system simulation and structural analysis to verify the plant performance and damage. If the results are satisfactory, the synthesis of an optimal policy for open-loop control is completed. Otherwise, the damage constraints should be revised and the optimization procedure is repeated to find another control sequence $\{u_k\}$. It is possible that an optimal solution may not exist due to overly stringent damage constraints. In that case, modifications of the constraints β or Γ or the cost functional J are needed. If none of these modifications are advisable, revision of the damage model or plant model should be considered. For example, an alternative approach such as fatigue crack growth model may be adopted in lieu of the cyclic strain approach for damage modeling (see Appendix B of the first part, Ray et al. (1993)).

In this research, a general purpose nonlinear programming package, namely the IMSL subroutine DNCONF, has been adopted to solve the nonlinear optimization problem. Other packages such as NPSOL (Gill et al., 1991) of Stanford University are being considered for improving the computational efficiency. Following the optimization procedure in Fig. 1, simulation experiments were carried out to evaluate the efficacy of the proposed damage-mitigating control as presented in the next section.

3 Simulation Results and Discussion

The damage mitigation concept, described in the first part, is verified by simulation experiments for open-loop control of a reusable rocket propulsion engine such as one described in (Sutton, 1992; Duyar et al., 1991). The plant model under control is a simplified representation of the dynamic characteristics of a bipropellant rocket engine as shown schematically in Fig. 2. The preburner serves as a gas generator for driving the liquid hydrogen (LH_2)-fuel turbopump. In this model, oxidant is separately supplied to the preburner and the main combustor chamber. Standard lumped parameter methods have been used to model the nonlinear plant dynamics in state-space form where the plant state vector consists

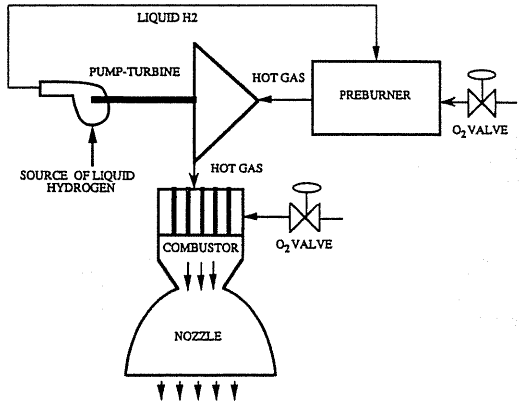

Fig. 2 Schematic diagram of a bipropellant rocket engine

of turbine shaft speed, pump (LH_2-fuel) mass flow rate, preburner gas pressure, preburner gas density, combustor gas pressure, combustor gas density, and the positions of the two oxidant flow valves. The critical plant output variables are combustor gas pressure and the oxidant/fuel (O_2/H_2) ratio, and the control inputs are commands for manipulation of the two oxidant valves. The structural model, as shown in Fig. 1 of the first part (Ray et al., 1993) and Fig. A.1 of Appendix A, represents the cyclic mechanical stresses at the root of a typical turbine blade that is presumed to be a critical component. The blade is represented by a three-node beam model with six degrees of freedom at each node while the first node is kept fixed. The load on the blade is assumed to consist of two components. The first component is due to the (time-dependent) drive torque which is derived as an output of the plant model. The second component is a dynamic term which represents the oscillatory load on the blade as it passes each stator. It is the second component that causes high cycle fatigue at the root of the blade while the first component is largely responsible for the mean stress. The fatigue damage model formulated in the first part was used to generate the results in Figs. 3 to 7.

The purpose of this simulation study is to examine the dynamic performance and damage of the nominal plant when the oxidant valves are manipulated to vary the engine thrust according to the open-loop control policy developed in Section 2. To demonstrate the broad concepts of fatigue damage mitigation, the nominal plant model was used in these simulation experiments with exact initial conditions and no disturbances and noise. However, if these conditions are not met, additional feedback control will be necessary because the open-loop control alone would be inadequate as discussed in Appendix A. Following the structure in Eq. (3), the cost functional J for nonlinear programming was selected to generate the open-loop control policy as:

$$J = \sum_{k=0}^{N-1} [\tilde{x}_k^T Q \tilde{x}_k + \dot{v}_k^T S \dot{v}_k + \tilde{u}_k^T R \tilde{u}_k + W(O_2/H_2)k^2] \tag{5}$$

where the deviations, $\tilde{x}_k$ and $\tilde{u}_k$, in the plant state vector and the control input vector are as defined in Eq. (3); and the diagonal matrices Q,S,R, and the scalar W serve as relative weights of the individual variables. Since the rocket engine performance is very sensitive to the oxidant/fuel (O_2/H_2) ratio, it was brought into the cost functional in Eq. (5) to prevent any large deviations from the desired value of 6.02

Table 1 The constraints for the two cases under simulation condition 1

Time	Constrained Case 1	Constrained Case 2
0 ms to 2 ms	$1.0 \times 10^{-6}\ s^{-1}$	$0.2 \times 10^{-6}\ s^{-1}$
2 ms to 3 ms	$2.5 \times 10^{-6}\ s^{-1}$	$0.5 \times 10^{-6}\ s^{-1}$
3 ms to 50 ms	$5.0 \times 10^{-6}\ s^{-1}$	$1.0 \times 10^{-6}\ s^{-1}$

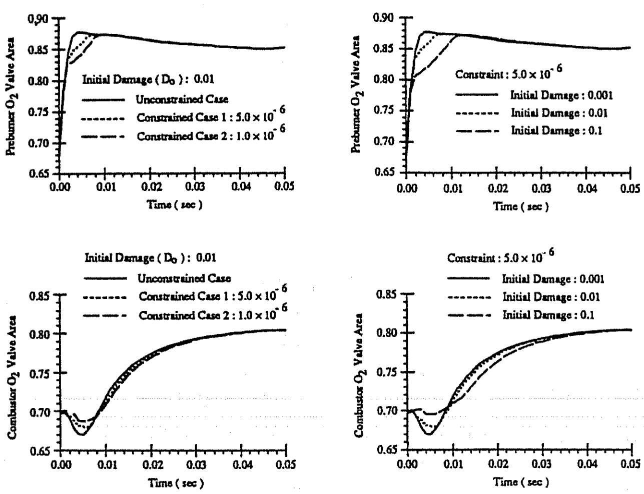

Fig. 3 Transient responses of the oxidant valve areas

through the transients. The simulation results in Figs. 3 to 7 were obtained under the following conditions:

Chamber Pressure Weight $Q_{55} = 12$; and all other weights $Q_{ii} = 1$, $i \neq 5$,

Control input weight $R = I$ where I is the identity matrix,

Damage Rate Weight $S = 0$; and O_2/H_2 ratio weight $W = 10$,

The rocket engine model is initiated from an initial equilibrium condition at 2700 psi chamber pressure and O_2/H_2 ratio of 6.02. From this condition the optimization procedure steers the plant to a new equilibrium position at 3000 psi and the same O_2/H_2 ratio of 6.02 in 50 milliseconds. The control commands to the two oxidant valves, are updated at every one millisecond. That is, N is equal to 50 in Eq. (5). The performance cost to be minimized is based on the deviations from the final equilibrium condition at 3000 psi. The results of simulation experiments for the two following conditions are presented as series of curves in the plates of Figs. 3 to 7:

Simulation Condition 1: Initial damage is set to $D_o = 0.01$; and unconstrained case; and two constrained cases in which the damage rate is constrained are listed in Table 1.

Simulation Condition 2: To examine the effects of nonlinear damage accumulation, simulation results are generated under three different initial values of the accumulated damage, namely, $D_o = 0.001$, 0.01 and 0.1 while the damage rate constraint is set identical to that of the constrained Case 1 in Table 1.

The transient responses in Figs. 3 to 7 examine the various engine variables under the above two simulation conditions. The plate in Fig. 3 shows the transient responses of the two oxygen valves resulting from the optimization over the time frame of 0 to 50 ms where the control action is updated at every millisecond. The corresponding changes in the oxidant flows are seen in Fig. 4 which also shows the transients of the fuel flow (i.e., liquid hydrogen). The responses of both control valves (and therefore the oxidant flows) become more restricted and sluggish as the damage rate constraint is made stronger. Similar effects are observed when the initial damage is increased. The rationale for this behavior is that, for a given stress amplitude, the damage rate increases with an increase in the initial damage. This dependence on the initial damage results from the γ-parameter in the nonlinear damage model (see Section 3.2 of the first part, Ray et al. (1993)), and does not occur in the linear damage model where γ is equal to 1. It is important to note that γ is greater than 1 in this study because the AISI 4340 steel used here is a high strength material.

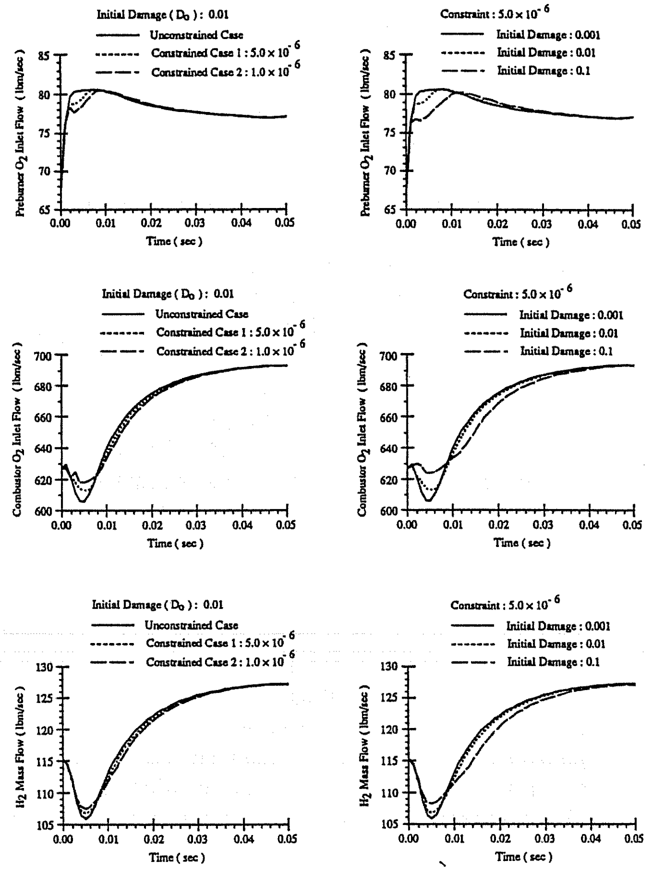

Fig. 4 Transient responses of oxidant and fuel flow rates

Figures 5 and 6 exhibit the effects of the varying oxygen inlet flow to the preburner and the main combustor on the engine dynamics. The resulting transients of the process variables, namely, O_2/H_2 ratio, and the pressure and temperature in the preburner and main combustion chamber, are shown for the two simulation conditions. As expected, for a given level of initial damage, both pressure and temperature dynamics tend to be slower as the constraint is made more severe. Similar effects are seen by increasing the initial value, D_o, of the accumulated damage. The combustor pressure is seen to rise monotonically in all cases after a small dip at about 2.5 ms while the preburner pressure keeps on increasing. These plots are largely similar except for the transients from 1 ms to 10 ms. Virtually all of fatigue damage accumulation in this transient operation takes place during this short interval as seen in the plate of Fig. 7. Furthermore,

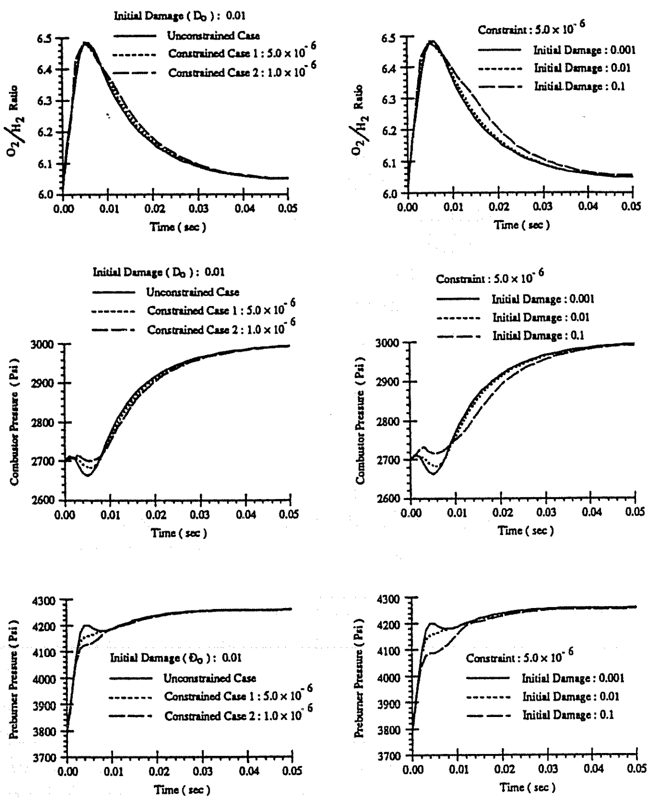

Fig. 5 Transient responses of preburner and combustor pressures

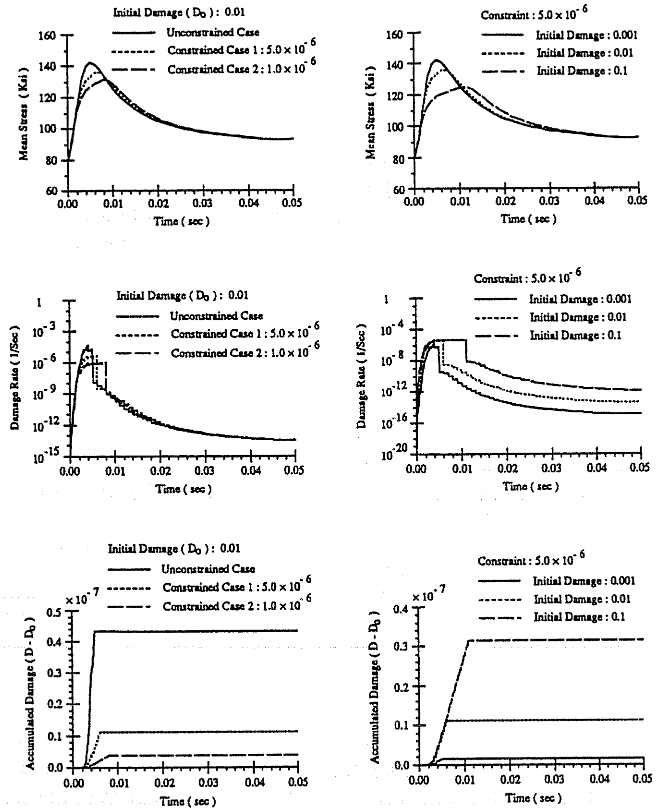

Fig. 7 Transient responses of damage rate and accumulated damage

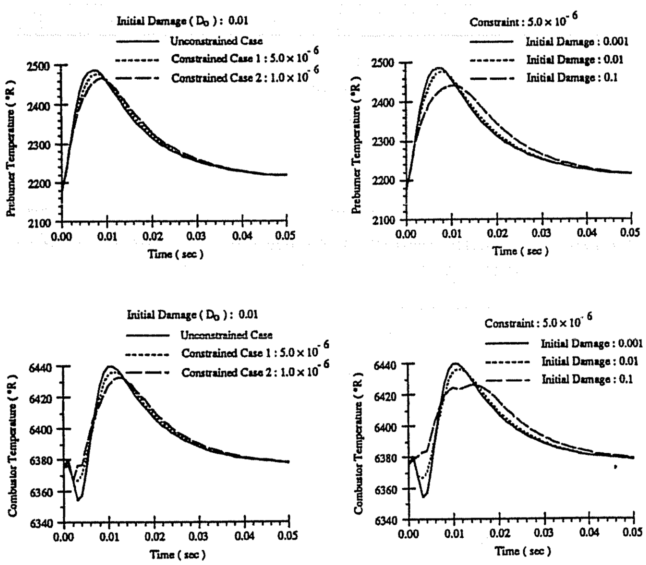

Fig. 6 Transient responses of preburner and combustor gas temperatures

the net excursion of the O_2/H_2 ratio is in the range of 6.0 to 6.5 in all cases for the up-thrust transient of the rocket engine. The peak value 6.5 of the mixture ratio is about the limit that would be tolerated during a transient excursion. The overshoot in the mixture ratio is caused by a drop in the hydrogen flow as seen in Fig. 4. At this point the turbopump demands more torque to increase its speed so that the pump pressure can be elevated to generate a higher value of hydrogen flow for the desired mixture ratio. This results in a peak overshoot in the mean stress as shown in Fig. 7. The sharp increase in stress is the cause of enhanced damage in the turbine blades.

Since the turbine blades are the critical components for damage analysis is in this study, the pressure ratio across the turbine, which directly influences the torque, is very important. For a given preburner pressure, as shown in Fig. 5, a reduction in the combustor pressure causes an increase in the turbine torque. It is the turbine torque and speed that set the cyclic stress and fatigue damage on the turbine blades. Therefore, the dip in the combustor pressure at about 2.5 ms is largely responsible for the peak mean stress displayed in Fig. 7. Both the mean stress and stress amplitude are the basic inputs to the damage model.

The graphs in Fig. 7 compare the damage rate and the accumulated damage for the two simulation conditions along with the transients responses of the mean stress. For the unconstrained case, the peak stress causes the largest overshoot in the damage rate which is plotted on a logarithmic scale. In contrast, for the initial damage of 0.001, the damage rate is within the limit of the constraint even though the peak of mean stress is the largest. This phenomenon is a result of a relatively small slope of the damage curve at the initial stages of the fatigue life. The accumulated damage, plotted on a linear scale, is seen to be significantly influenced by the constraints and also by the initial damage. This suggests that, for reusable rocket engines, the constraints need to be appropriately specified based on the knowledge of the initial damage. The damage rate is dependent on the two sequences of control commands, and the oxidant flows into the preburner and combustor are changed in response. Therefore, if the initial damage cannot be accurately assessed, then it might be safe to generate the control command sequences on the assumption of a conservative, i.e., larger, value of the initial damage at the expense of the engine performance.

The important observation in these simulation experiments is the substantial reduction in the accumulated damage, thereby extending the service life of the turbopump. The accumulated damage in the unconstrained case is seen to be about four to twelve times that of the constrained case. This is a clear message that the consideration of damage in the control of transients to which a rocket engine is exposed can have a considerable impact on the life of critical components (in this case, the turbine blades). It is noted that there is practically insignificant penalty in the response times of the chamber pressure, i.e., the engine thrust, between the unconstrained and the constrained cases. If one is willing to pay a small price in response time, much larger gains on damage accumulation can be achieved.

Figures 3 to 7 exemplify the effects of upthrust transients during a short period of 50 ms. Complete operations of a rocket engine during a single flight include many such upthrust transients, and the steady-state operation may last for several hundreds of seconds. Although the damage rate during the steady state is much smaller than that during a transient operation, the total damage accumulation during the steady state may not be relatively insignificant. Therefore, during one flight of a (reusable) rocket engine, the cumulative effects of the transient and steady state operations need to be considered for estimation of total accumulated damage.

The simulation experiments, described above, only consider a single point of critical stress, namely, the turbine blades. In this case, the damage vector is one-dimensional. Simultaneous control of damage at several other critical areas in the rocket engine, such as the nozzle lining, shall render the damage vector to be multi-dimensional. The optimization problem is then to generate control sequences that will not only make a trade-off between the performance and damage but also strike a balance between potentially conflicting requirements of damage mitigation at the individual critical points.

4 Summary, Conclusions, and Applications

The theme of the research in damage-mitigating control of mechanical systems, as reported in this two-part paper, is summarized as follows:

- For control of mechanical systems, on-line damage prediction and damage mitigation are carried out based on the available sensory and operational information such that the plant can be inexpensively maintained, and safely and efficiently steered under diverse operating conditions.
- High performance is achieved without overstraining the mechanical structures such that the functional life of critical components is increased resulting in enhanced safety, operational reliability, and availability.

In this paper we have developed a continuous-time model of fatigue damage that can be integrated with the plant dynamic model for the purpose of control synthesis and failure prognosis. A procedure for synthesizing an optimal policy for open-loop control has been formulated. Finally, efficacy of the proposed damage-mitigating control has been demonstrated via simulation to show how the durability of a reusable rocket engine can be increased.

This ongoing research in damage-mitigating control addresses interdisciplinary work in the fields of active control technology and structural integrity, particularly as applied to fatigue life. Extended life coupled with enhanced safety and high performance will have a significant economic impact in diverse industrial applications. Furthermore, as the science and technology of materials evolve, the damage characteristics of the structural components can be systematically incorporated within the framework of the proposed control system.

Applications of damage-mitigating control of mechanical systems include a wide spectrum of engineering applications such as reusable rocket engines for space propulsion, rotating and fixed wing aircraft, fossil and nuclear plants for electric power generation, automotive and truck engine/transmission systems, and large rolling mills. In each of these systems, damage-mitigating control can enhance safety and productivity accompanied by reduced life cycle cost. For example, the availability of power plants often suffers from premature failures of steam generator tubes (due to corrosion-fatigue and creep), main steam and reheat steam pipelines (due to creep and fatigue), condensor tubes (due to stress corrosion cracking and flow-induced vibration) and low pressue turbine blades (due to stress corrosion, erosion, and fatigue). A continuous-time damage model will allow timely warnings of these failures, and the resulting decision and control actions will not only avoid an early shutdown but also improve maintainability. In the load following mode of a fossil power plant, excursions of the main steam and reheat steam pressure and temperature must be regulated within prescribed limits to ensure plant safety (e.g., protection of the steam turbines). This is usually achieved by manipulating the feed water flow and the fuel flow actuators. However, following a command of load change (Ray and Berkowitz, 1979), an abrupt reduction of feed water flow or an abrupt increase of the fuel flow could overheat the steam generator tubes. Repeated occurrences of tube overheating could result in creep-fatigue failures. Such incidents could be alleviated by a relatively small reduction in plant performance if the control system is structured with the capability of predicting these impending failures and thereby exercising authority over the lower level control modules. A more complex application of the damage mitigation concept is the start-up and scheduled shutdown of rocket engines and power plants, and take-off and landing of commercial aircraft, in which the damage information can be utilized for real-time plant control either in the fully automated mode or with human operator(s) in the loop. Another example is the control of automotive engine and transmission systems to reduce stresses in the drive-train components without comprising driving performance and comfort. The result will be a combination of extended life and reduced drive-train mass with associated savings in the fuel consumption.

Acknowledgments

The authors acknowledge benefits of discussion with Professor D. A. Koss regarding the metallurgical aspects of the research work and technical contributions of Dr. L-W. Liou during the initial phase of this project.

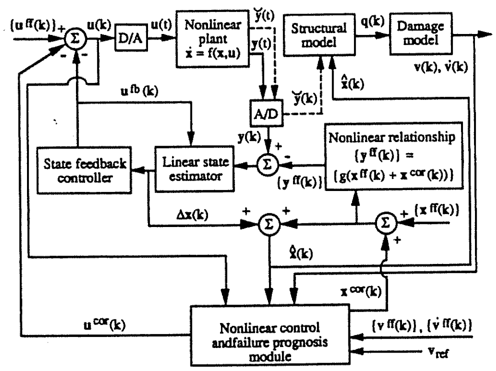

Fig. A.1 Closed-loop damage control and failure prognosis system

APPENDIX A

Closed-Loop Control Policy

Nonlinear programming generates an open-loop control policy to achieve optimal performance under the specified constraints of damage rate and accumulated damage. However, because of plant modeling uncertainties (including unmodeled dynamics), sensor noise, and disturbances, the actual plant response shall deviate from that of the modeled system when the plant is excited by the sequence of open-loop control commands. Therefore, a closed-loop control system is necessary to compensate for these deviations, and an output feedback controller may serve this purpose. A block diagram of the closed-loop damage control and failure prognosis system is proposed in Fig. A.1 where $\{u^{ff}\}$, $\{x^{ff}\}$, $\{\nu^{ff}\}$ and $\{\dot{\nu}^{ff}\}$ represent the sequences of the plant input, plant state, accumulated damage, and damage rate, respectively, generated as an optimal solution of the open-loop control problem via nonlinear programming, and $\{y^{ff}\}$ is the resulting sequence of plant output, which is obtained as a nonlinear function $g(\cdot)$ of the plant state vector x^{ff}. The trajectory of the actual plant output y should be close to that of the desired plant output y^{ff} which serves as the reference trajectory. The resulting error in the plant output is an input to the state estimator, and the feedback control signal u^{fb} compensates for errors resulting from plant disturbances and sensor noise. The estimated state $\hat{x}$ which is obtained as the sum of the estimated state error and the reference state x^{ff} is fed to the structural model. The output of the structural model is the load vector q which contains stress, strain and other information necessary for damage assessment. Some of the elements of the load vector q (e.g., strain and temperature at the critical points) may be directly measurable as indicated in Fig. A.1 by additional measurements $\check{y}$.

The closed-loop control system is partitioned into two modules. The state feedback control law in the first module could be formulated by using the established techniques of robust multi-input multi-output (MIMO) control synthesis, which rely on approximation of the plant dynamics by a linear time-invariant model (e.g., H_2-based LQG/LTR (Stein and Athans, 1987), H_2/H_∞ optimization (Doyle et al., 1989) or μ-synthesis (Packard and Doyle, 1993; Stein and Doyle, 1991; Skogestad et al., 1988). However, if the plant dynamics cannot be approximated by piecewise linearization or time-averaging of the varying parameters, then selection of the control synthesis technique will depend upon the specific application. The second module is a nonlinear controller which contributes to damage reduction in the critical plant components under feedback control and also serves to generate early warnings and prognoses of impending failures of the critical plant components. Since the damage rate $\dot{\nu}$ in the closed-loop control system may violate the specified constraints due to the additional compensation generated by the feedback control effort u^{fb}, a nonlinear controller is incorporated into the system to reduce the damage rate $\dot{\nu}$. This is accomplished by corrections x^{cor} in the reference trajectory and u^{cor} in the control effort. The rationale for modifying the reference trajectory $\{x^{ff}\}$ is that, due to plant disturbances and sensor noise, it may not be possible to follow this trajectory without violating the damage constraints. The additional control effort u^{cor} is intended to provide a fast corrective action to the control input u_k, whenever necessary. The nonlinear control system in the outer loop, as shown in Fig. A.1, serves two purposes, namely, (i) trimming of the linear feedback control signal to maintain the damage rate or accumulated damage rate vector within the limits, and (ii) modification of the tracking signal (i.e., the reference signal) to circumvent the problem of exceeding the damage rate limits, which may result from plant modeling errors, uncertainties and disturbances. A possible approach to synthesis of the nonlinear damage controller is first to postulate a mathematical structure of the controller and then optimize the controller parameters relative to a cost functional that would penalize:

- Plant state and damage rate over the task period;
- Final plant state and the accumulated damage.

The outputs of the damage controller, namely x^{cor} and u^{cor} in Fig. A.1, need to be constrained to be norm-bounded to assure the system stability; x^{cor} and u^{cor} can also be considered as exogenous inputs to the linear robust control system in the inner loop. Therefore, the bounds on x^{cor} and u^{cor} can be fine-tuned to satisfy the specified requirements of performance and stability robustness in the μ-synthesis procedure.

APPENDIX B

Failure Prognosis and Risk Analysis

Traditionally, the risk index and residual service life (Bolotin, 1989) of mechanical structures and machine components are calculated off-line on the basis of statistical models of the mechanical properties of the material, operating conditions, disrupting, and accidents (e.g., seismic and large atmospheric disturbances). It follows from Eq. (2) that the service life is finite as the damage accumulation is monotonic with time. Furthermore, the plant operations and maintenance are scheduled on the basis of the fact that the damage accumulation is likely to be accelerated in the event of accidents or disruptions. Therefore, on-line monitoring of the accumulated damage will allow refinements of the risk index and residual service life estimates (Bogdonoff and Kozin, 1985; Sobczyk and Spencer, 1992) as time progresses. Specifically, predictions of the accumulated damage and the current damage rate will assist the plant engineer in making dynamic decisions regarding the safety procedures, mission accomplishments, and the time interval between major maintenance actions. The concept of service life evaluation via on-line monitoring is outlined below.

Let $\phi_j(t)$, $j = 0, 1, 2, \cdots, m$ represent predicted occurrences of impending accidents or major disruptions after the current instant of time, t, such that the set ϕ_0 indicates the absence of any accidents or disruptions, and the event sets ϕ_j, $j = 0, 1, 2, \cdots, m$ are exhaustive and mutually exclusive. Then, in the absence of any accidents or disruptions, the service life θ_0 at time t is obtained in the deterministic setting in terms of the plant state estimate $\hat{x}(t)$ and damage state $\nu(t)$ as:

$$\theta_o(t,\hat{x}(t),\nu(t)) = \mathrm{Sup}\{\tau \in [t,\infty) \text{ such that } \nu(\tau) \in \Omega \text{ conditioned on occurrence of } \phi_o(t)\} \quad (B.1)$$

where Ω is the set of the admissible damage vectors for the plant to remain in service. Obviously, the service life may be reduced if an accident or disruption occurs. That is, $\theta_j \leq \theta_0$ for $j = 1, 2, \cdots, m$. Hence, the service life θ_j based on the occurrence of the event $\varphi_j(t)$ is obtained in the probabilistic setting as:

$$\theta_j(t,\hat{x}(t),\nu(t)) = \mathrm{Sup}\{\tau \in [t,\theta_0] \text{ such that } Pr\{\nu(\tau) \in \Omega | \varphi_j(t)\} \geq (1-P)\}, \quad j = 1, 2, \cdots, m \quad (B.2)$$

where $0<P<1$ is the threshold probability that the damage vector may violate the admissible set Ω during the service period, i.e., while the plant is in operation. Then, the expected service life at time, t, can be obtained as:

$$\Theta(t,\hat{x}(t),\nu(t)) = \sum_{j=0}^{m} \theta_j(t,\hat{x}(t),\nu(t))\, \pi_j(t) \quad (B.3)$$

where $\pi_j(t)$, $j = 1, 2, \cdots, m$ are the *a priori* probabilities of occurrence of the events ϕ_j over the interval $[t, \theta_0]$.

In the absence of any accident or disruption during the period remaining after the current time t, the service life θ_0 in Eq. (B.1) can be obtained by solving Eqs. (1) and (2) in Section 2. However, computation of θ_j for $j = 1, 2, \cdots, m$ in Eq. (B.2) is not straightforward because the damage accumulation depends not only on the variations in the plant and damage dynamics as a result of the accident or disruption but also on the instant(s) of its occurrence. To predict the service life from Eq. (B.2), probabilistic risk analysis is necessary beyond those reported in literature (Bolotin, 1989; Bogdonoff and Kozin, 1985; Sobczyk and Spencer, 1992). This would require nonlinear stochastic modeling of the plant and damage dynamics. Since analytical solutions of the nonlinear stochastic differential equations excited by randomly occurring discrete events may not be achievable, the idea is to generate approximate solutions from simplified models supported by the available sensor data history. These results, in turn, are to be verified by simulation.

The major implications of the proposed service life prediction and risk analysis are: (1) generation of early warnings resulting in diminished risk of loss of human life and plant equipment; (ii) enhancement of plant availability by avoiding an emergency shutdown; and (iii) reduction of the plant operational cost by dynamic rescheduling of the maintenance plan via on-line assessment of damage in the critical components.

References

Bogdonoff, J. L., and Kozin, F., 1985, *Probabilistic Models of Cumulative Damage*, Wiley Interscience, New York.

Bolotin, V. V., 1989, *Prediction of Service Life for Machines and Structures*, ASME.

Doyle, J. C., Glover, K., Khargonekar, P., and Francis, B., 1989, "State-Space Solutions to Standard H_2 and H_∞ Control Problems," *IEEE Transactions on Automatic Control*. Vol. 34, No. 8, Aug., pp. 831–847.

Duyar, A., Eldem, V., Merrill, W. C., and Guo, T-H., 1991, "State Space Representation of the Open-Loop Dynamics of the Space Shuttle Main Engine," *ASME* JOURNAL OF DYNAMIC SYSTEMS, MEASUREMENT, AND CONTROL. Vol. 113, Dec., pp. 684–690.

Gill, P. E., Murray, W., Saunders, M. A., and Wright, M. H., 1991, NPSOL Version 4.06, Software Distribution Center, Stanford University, Palo Alto, CA.

Isermann, R., 1984, "Process Fault Detection Based on Modeling and Estimation Methods," *Automatica*, Vol. 20, No. 4, pp. 387–404.

Lorenzo, C. F., and Merrill, W. C., 1991, "An Intelligent Control System for Rocket Engines: Need, Vision, and Issues," *IEEE Control Systems Magazine*, Vol. 11, No. 1, June, pp. 42–46.

Luenberger, D. G., 1984, *Linear and Nonlinear Programming*, Addison-Wesley, Menlo Park, CA.

Packard, A., Doyle, J., and Balas, G., 1993, "Linear Multivariable Robust Control with a m Perspective," *ASME* JOURNAL OF DYNAMIC SYSTEMS, MEASUREMENT, AND CONTROL, 50th Anniversary Issue, Vol. 115, June, pp. 428–438.

Ray, A. and Berkowitz, D. A., 1979, "Design of a Practical Controller for a Commercial Scale Fossil Power Plant," *ASME* JOURNAL OF DYNAMIC SYSTEMS, MEASUREMENT, AND CONTROL, Dec., pp. 284–289.

Ray, A., Wu, M-K., Carpino, M., and Lorenzo, C. F., 1993, "Damage-Mitigating Control of Mechanical Systems: Part I—Conceptual Development and Model Formulation," published in this issue, pp. 437–447.

Skogestad, S., Morari, M., and Doyle, J. C., 1988, "Robust Control of Ill-Conditioned Plants: High Purity Distillation," *IEEE Transactions on Automatic Control*, Vol. 33, No. 12, Dec., pp. 1092–1105.

Sobczyk, K., and Spencer, B. F., Jr., 1992, *Random Fatigue: Data to Theory*, Academic Press, Boston, MA.

Stein, G., and Athans, M. A., 1987, "The LQG/LTR Procedure for Multivariable Feedback Control Design," *IEEE Transactions on Automatic Control*, Vol. AC-32, No. 2, Feb., pp. 105–114.

Stein, G. and Doyle, J. C., 1991, "Beyond Singular Values and Loop Shapes," *IAIAA Journal of Guidance, Control and Dynamics*, Vol. 14, No. 2, Feb., pp. 105–114.

Sutton, G. P., 1992, *Rocket Propulsion Elements*, Wiley Interscience, New York.

Vidyasagar, M., 1992, *Nonlinear Systems Analysis*, 2nd ed., Prentice Hall, Englewood Cliffs, NJ.

Wu, M-K., 1993, Damage-Mitigating Control of Mechanical Systems, Ph.D. Dissertation in Mechanical Engineering, The Pennsylvania State University, University Park, PA.